Cancer & Metabolism

RESEARCH Open Access

GDF15-mediated enhancement of the Warburg effect sustains multiple myeloma growth via TGFβ signaling pathway

Wenjing Xue[1], Ying Li[1], Yanna Ma[1] and Feng Zhang[2*]

Abstract

The Warburg effect, characterized by the shift toward aerobic glycolysis, is closely associated with the onset and advancement of tumors, including multiple myeloma (MM). Nevertheless, the specific regulatory mechanisms of glycolysis in MM and its functional role remain unclear. In this study, we identified that growth differentiation factor 15 (GDF15) is a glycolytic regulator, and GDF15 is highly expressed in MM cells and patient samples. Through gain-of-function and loss-of-function experiments, we demonstrated that GDF15 promotes MM cell proliferation and inhibits apoptosis. Moreover, GDF15 enhances Warburg-like metabolism in MM cells, as evidenced by increased glucose uptake, lactate production, and extracellular acidification rate, while reducing oxidative phosphorylation. Importantly, the tumor-promoting effects of GDF15 in MM cells are fermentation-dependent. Mechanistically, GDF15 was found to promote the expression of key glycolytic genes, particularly the glucose transporter GLUT1, through the activation of the TGFβ signaling pathway. Pharmacological inhibition of the TGFβ signaling pathway effectively abrogated the oncogenic activities of GDF15 in MM cells, including cell proliferation, apoptosis, and fermentation. In vivo experiments using a subcutaneous xenotransplanted tumor model confirmed that GDF15 knockdown led to a significant reduction in tumor growth, while GDF15 overexpression promoted tumor growth. Overall, our study provides insights into the molecular mechanisms underlying MM pathogenesis and highlights the potential of targeting GDF15-TGFβ signaling -glycolysis axis as a therapeutic approach for future therapeutic interventions in MM.

Keywords Multiple myeloma, Warburg effect, GDF15, Transforming growth factor-beta

Introduction

The reprogrammed metabolism is a distinct feature of cancer and plays a significant role in the initiation and progression of tumors. Unlike normal differentiated cells, which primarily utilize oxidative phosphorylation for energy production, cancer cells rely on the glycolytic pathway to generate ATP, even in the presence of sufficient oxygen. This metabolic phenomenon is referred to as "aerobic glycolysis" or the "Warburg effect" [1]. The shift from oxidative phosphorylation to glycolysis leads to increased glucose consumption, lactate release, and provides essential support for the rapid proliferation of

*Correspondence:
Feng Zhang
zfxwj0992@sina.com
[1]Department of Hematology, Jinshan Hospital, Fudan University, Shanghai 201508, China
[2]Department of Cardiovascular medicine, Jinshan Hospital, Fudan University, Shanghai 201508, China

cancer cells by supplying ample cellular building blocks [2, 3]. Consequently, numerous studies have suggested that targeting aerobic glycolysis holds promise as a therapeutic approach for treatment [4, 5].

Multiple myeloma (MM) is a type of cancer that originates from plasma cells and accounts for approximately 10% of all hematological neoplasms [6–8]. The disease is characterized by symptoms such as hypercalcemia, painful bone lesions, kidney damage, anemia, and weight loss [9, 10]. Currently, the primary treatment for MM involves stem cell transplantation [7, 11]. However, for patients who are not suitable candidates for this procedure or those with recurrent MM, chemotherapy options such as proteasome inhibitors and immunomodulators are available [12, 13]. While these treatment approaches have notably improved the median progression-free survival, MM remains incurable, largely due to incomplete understanding of the biological processes underlying the disease. Therefore, it is crucial to elucidate the exact pathogenesis of MM.

Growth differentiation factor 15 (GDF15) belongs to the transforming growth factor-β (TGFβ) superfamily [14]. It exists as a homodimer, consisting of two polypeptide chains with 112 amino acids, connected by an interchain disulfide bond. GDF15 is expressed at low levels in most tissues under physiological conditions. However, in various pathological processes such as inflammation, injury, and cancer, the expression of GDF15 is significantly up-regulated, and it plays a role in regulating these disease processes [15–19]. For example, GDF15 expression is induced during cancer cachexia, and neutralizing GDF15 has been shown to effectively reverse body weight loss and restore physical performance [20]. In the context of MM, GDF15 expression is notably increased in MM patients compared to controls [21]. Elevated levels of GDF15 have been associated with advanced MM disease stage, anemia, and inflammation [22]. Despite these associations, the precise molecular mechanisms through which GDF15 operates in MM remain largely unknown.

In this study, we performed differential analysis in MM and confirmed the overexpression pattern of GDF15. Notably, we have uncovered a previously unrecognized role of GDF15 in modulating the Warburg effect of MM cells. Furthermore, we have observed that GDF15 is capable of activating the TGFβ signaling pathway, leading to the transcriptional induction of glycolytic genes, particularly the glucose transporter GLUT1, thereby enhancing *fermentation*. We have also found that genetic silencing of GDF15 effectively inhibits MM progression both in vitro and in vivo.

Materials and methods

Cells and reagents

The MM cell lines (ARP1, H929, KMS-11, LP-1, RPMI8826, and U266) were acquired from the American Type Culture Collection and the Shanghai Cell Bank (Chinese Academy of Science, Shanghai, China). Prior to experiments, the cell lines underwent authentication through STR profiling. Primary MM cells were isolated from bone marrow aspirates from MM patients using anti-CD138 antibody-coated magnetic beads (Miltenyi Biotec, Germany). Peripheral blood mononuclear cells (PBMC) were obtained from fresh buffy coats from healthy donors. All MM cells were cultured in RPMI-1640 or IMEM (Gibco) supplemented with 10% fetal bovine serum (FBS) and 1% penicillin/streptomycin under standard cell culture conditions (37 °C, 5% CO2). Patient samples were obtained from the Department of Hematology of Jinshan Hospital, Fudan University, during the period from January 2022 to December 2023. The procedures followed medical-ethics approval practices. Recombinant human GDF15 (rGDF15; 228-12036) was purchased from RayBiotech (Norcross, GA, USA). Recombinant human TGFβ (7754-BH) was obtained from R&D Systems (Minneapolis, MN, USA). LY2109761, a TGFβ receptor inhibitor, was obtained from a biochemical company (S2704; Selleck, USA).

Animal experiments

For the in vivo assays, 8-week-old male B-NDG mice were obtained from Biocytogen Co., Ltd. (Jiangsu Province, China). The mice were housed in a specific pathogen-free environment in full compliance with institutional policies. They were randomly divided into four groups, with five repeats for each group: RPMI8826-shNC and RPMI8826-shGDF15, H929-OE-vector and H929-OE-GDF15. Each mouse received a subcutaneous injection of 1×10^6 cells. The development and progression of solid tumors was longitudinally monitored over 4 weeks. Tumor volume (V) was calculated twice a week using the formula: $V = (\text{length} \times \text{width}^2)/2$. This study was reviewed, approved, and supervised by the Institutional Animal Care and Use Committee of Fudan University.

shRNA and overexpression experiments

GDF15-targeting shRNAs for MM cells (sh-*GDF15*-#1, sh-*GDF15*-#2, sh-*GDF15*-#3) and its negative control (sh-NC) were designed and synthesized by GenePharma Technology Co., Ltd. (Shanghai, China). The sequences for *GDF15*-targeting shRNAs were: sh-*GDF15*-#1, GCT ACAATCCCATGGTGCTCA; sh-*GDF15*-#2, GCCAA AGACTGCCACTGCATA; sh-*GDF15*-#3, GCCCAAA CAGCTGTATTTATA. Full coding sequence of human *GDF15* gene or control sequence was cloned into pcDNA 3.1 plasmids to generate pcDNA 3.1-*GDF15* (OE-*GDF15*)

and pcDNA 3.1-NC vector (OE-vector), respectively. To package the virus, 293T cells were used along with virus packaging auxiliary plasmids psPAX2 and pMD2G. 24 h prior to transfection, 5×10^6 293T cells were seeded onto each 100 mm culture plate. A mixture of 12 μg of target plasmid, 9 μg of psPAX2 and 3 μg pMD2G in 500 μl of OPTI-MEM was prepared and left at room temperature for 5 min. Additionally, 6 0 μl PEI (Cat#: 408727, Sigma) was dissolved in 500 μl serum-free medium, left at room temperature for 5 min, and then mixed with the previous tube. After 20 min at room temperature, the mixture was added to the Petri dish and cultured under 37 °C and 5% CO_2 After 6 h, the culture medium was replaced with complete medium, and the culture was continued for 48 h. The supernatant was collected into a 15 ml centrifuge tube and stored at 4 °C. The lentivirus supernatant was filtered with a 0.45 μm filter, centrifuged at 80,000 g at 4 °C for 6 h, and the supernatant was discarded. Finally, 200 μl of culture medium was added to each dish of cells to dissolve the lentivirus precipitate. The virus was diluted to 200 times with fresh culture solution, and 8 μg/ml of polybrene was added. The cells were then infected for 8 h, after which the fresh culture was replaced and the cells were incubated for 72 h. The interference efficiency was detected by PCR and western blotting.

Cell proliferation assay

Cell proliferation was examined using the CCK-8 assay. Specifically, 2×10^3 indicated MM cells were seeded onto 96-well plates per well and cultured overnight at 37 °C. At 24, 48, 72, and 96 h, 10 μl of CCK-8 solution was added to each well. After incubation for 1.5 h, the absorbance at 450 nm was detected using a microplate reader (BioTek).

Apoptosis analysis by flow cytometry

The detection of apoptotic cells was carried out using Annexin V-FITC/PI staining. Cultured MM cells (5×10^5 cells/sample) were harvested, washed with cold PBS, and then resuspended in 400 μL of Annexin binding buffer. Following this, 5 μL of annexin V-FITC and 5 μL of PI (BD Pharmingen; BD Biosciences) were added to each sample. After thorough mixing, the samples were incubated for 20 min in the dark at room temperature. Subsequently, the stained samples were subjected to measurement using flow cytometry within 1 h. and the resulting data were analyzed using the BD FACSCalibur System.

Glucose uptake and lactate production measurements

The glucose and lactate levels in the culture medium were measured using a glucose uptake assay kit (colorimetric, Abcam, ab136955) and a lactate assay kit (Biovision, CA; K607-100), respectively, following the manufacturers' instructions. Subsequently, the glucose uptake and lactate release were normalized to the total protein level of each sample.

Seahorse experiments

The glycolytic flux (extracellular acidification rate, ECAR) and respiratory capacity (oxygen consumption rate, OCR) analyses of MM cells (RPMI8226 and H929) were conducted using the Seahorse XF96 Extracellular Flux Analyzer from Seahorse Bioscience, Billerica, MA, USA. The myeloma cells were attached to the bottom of a 24-well plate using Cell-Tak cell and tissue adhesive from BD Biosciences. For the ECAR detection, glucose, ATP synthase inhibitor (oligomycin, O), and 2-Deoxy-D-glucose (2-DG) were added to the microplate, and the change in pH was monitored to reflect the glycolysis level of the cells. In the detection of OCR, ATP synthase inhibitor oligomycin, mitochondrial uncoupler FCCP, and antimycin A/rotenone (A&R) were added to the microplate, and the change in oxygen concentration was monitored. Finally, the ECAR and OCR data were normalized to the total protein level of each sample for analysis.

ELISA assay

The cell culture medium of different MM cells was harvested and prepared as a 10 times dilution. The commercial ELISA kits for human GDF15 (#DGD150) and mouse GDF15 (#MGD150) were obtained from R&D Systems (Minneapolis, MN, USA). The GDF15 level in the culture medium and tissue sample was then detected following the manufacturer's instructions provided with the ELISA kit.

RNA isolation and quantitative real-time PCR

Total RNA was extracted from MM cells and PBMC using Trizol from Invitrogen Life Technologies, Carlsbad, CA, USA, following the manufacturer's protocol. The concentration and A260/A280 of the RNA samples were measured using a NanoDrop spectrophotometer. The cDNA synthesis was carried out using the HiScript II 1st Strand cDNA Synthesis Kit (Cat. #R211-002, Vazyme). Real-time qPCR was performed with SYBR Green Master Mix (Cat. #HY-K0523, MedChemExpress) in an ABI7500 PCR instrument. ACTB was used as the endogenous reference gene for normalization. The primer sequences were as follows:

GDF15 forward, 5'-GACCCTCAGAGTTGCACTCC-3';
GDF15 reverse, 5'-GCCTGGTTAGCAGGTCCTC-3';
HK2 forward, 5'-TTGACCAGGAGATTGACATGGG-3';
HK2 reverse, 5'-CAACCGCATCAGGACCTCA-3';
PKM2 forward, 5'-ATAACGCCTACATGGAAAAGTGT-3';
PKM2 reverse, 5'-TAAGCCCATCATCCACGTAGA-3';

SLC2A1 forward, 5'-ATTGGCTCCGGTATCGTCAAC-3';
SLC2A1 reverse, 5'-GCTCAGATAGGACATCCAGGGTA-3';
LDHA forward, 5'-ATGGCAACTCTAAAGGATCAGC-3';
LDHA reverse, 5'-CCAACCCCAACAACTGTAATCT-3';
SMAD2 forward, 5'-TCATAGCTTGGATTTACAGCCAG-3';
SMAD2 reverse, 5'-TTCTACCGTGGCATTTCGGTT-3';
ACTB forward, 5'-CATGTACGTTGCTATCCAGGC-3';
ACTB reverse, 5'-CTCCTTAATGTCACGCACGAT-3'.

Western blotting

Total proteins were extracted from specified MM cells using RIPA lysis buffer containing protease and phosphatase inhibitors (P1261, Solarbio, China). The protein concentration was determined using the BCA Protein Assay Kit, followed by the addition of 5× SDS-PAGE Loading Buffer and heating at 95 °C for 5 min. For SDS-PAGE Electrophoresis, the protein samples were loaded onto a 15% acrylamide separation gel and subjected to electrophoresis at 70 V for 30 min, followed by 120 V for 60 min. Subsequently, a 250 mA constant current wet transfer was performed for 90 min. The membrane was then blocked with 5% skimmed milk powder at room temperature for 1 h, followed by overnight incubation with primary antibodies at 4 °C. The next day, after washing the membrane with TBST, the secondary antibody labeled with HRP (1:5000) was added and incubated at room temperature for 1 h. Following this, the membrane was washed with TBST and developed with chemiluminescence detection liquid (PK10003, Proteintech). Finally, the immunoblots were visualized using a GelDoc Go gel imaging system (Bio-Rad Company, America), with β-actin serving as the internal control. The following primary antibodies were used: GDF15 (27455-1-AP, Proteintech), PKM2 (#4053, Cell Signaling Technology), GLUT1 (21829-1-AP, Proteintech), LDHA (21799-1-AP, Proteintech), HK2 (66974-1-Ig, Proteintech), p-Smad2 (#18338, Cell Signaling Technology), Smad2 (#5339, Cell Signaling Technology), p-Smad3 (#9520, Cell Signaling Technology), Smad3 (#9523, Cell Signaling Technology), and β-actin (66009-1-Ig, Proteintech).

Chromatin immunoprecipitation (ChIP)

MM cells were seeded in a 6-mm dish at a density of 2×10^6 for the ChIP assay using the ChIP Assay kit (Thermo Fisher Scientific, USA) following the manufacturer's instructions. In brief, 37% formaldehyde was first added to crosslink proteins, and the reaction was terminated with 0.125 M glycine, followed by ultrasonic treatment. To determine the binding of SAMD2 to the promoter of *SLC2A1*, the chromatin-protein complex was immunoprecipitated with 5 μg anti-Smad2 antibody or 1 μg control IgG. The immunoprecipitated DNA was then amplified using specific primers to analyze the binding site of *SLC2A1* gene promoter. The *SLC2A1* promoter-specific primers were described as follows:

SLC2A1-prt-F1, 5'-CTGGTGCCATGAAGAAGGACCGTG-3';
SLC2A1-prt-R1, 5'-CAAGGCTTCAATTCCTGTGGTCTC-3';
SLC2A1-prt-F2, 5'-GGATCACGAGGTCAAGAGTTCAAGA-3';
SLC2A1-prt-R2, 5'-CATTAAGGACATGATAGACCTCG-3';
SLC2A1-prt-F3, 5'-GAGAACGAGCCGATCGGCAGCC-3';
SLC2A1-prt-R3, 5'-GCCATTGGCTGGCGACGCCGGTG-3';
SLC2A1-prt-F4, 5'-GCAGGAGACCAAACGACGGGGGTC-3';
SLC2A1-prt-R4, 5'-CAGCGCTGCGCTGGTGGCTCTGG-3'.

Luciferase reporter assay

The PCR product of different *SLC2A1* promoter regions was inserted into a pGL3-Basic plasmid. MM cells were then seeded into 24-well plates at a density of 2×10^5 cells per well. When the cells reached 70–80% confluence, the reporter gene plasmid and pRL-TK (internal control plasmid) were co-transfected into the cells. After 24 h culture, the cells were collected, and the luciferase and Renilla reporter signals were detected using a dual-luciferase reporter kit (Promega Luciferase Assay System E1501). Finally, the ratio of firefly luciferase to Renilla luciferase for each group was calculated as a measure of promoter activity.

Statistical analysis

The differentially expressed genes were identified based on a published dataset deposited to GEO datasets under the accession number GSE6477. All data are presented as mean ± SD and are representative of three independent experiments. Statistical significance was determined using GraphPad Prism (San Diego, CA) with two-tailed unpaired Student t-tests for comparison of two groups and one-way ANOVA for comparison of more than two groups. P values less than 0.05 were considered statistically significant.

Results

GDF15 is identified as a differentially expressed gene in MM

Initially, to identify the critical genes involved in MM, we analyzed the gene expression data of plasma cells from MM patients. We selected the GEO series 6477 (GSE6477) [23], which includes newly diagnosed MM ($n=75$), relapsed MM ($n=28$), the precancerous states monoclonal gammopathy of undetermined significance (MGUS, $n=21$), and normal donor samples ($n=15$) for our analysis. Among the genes with the largest fold change (Top 10), we found *GDF15* to be of particular interest due to its lower p-value and false discovery ratio (FDR) (Fig. 1A). GDF15 expression levels did not differ

A

gene	pvalue	fdr	log2FC	High.Ave	Low.Ave
RPS4Y1	0.088	0.475	3.478	3919.402	3254.715
DDX3Y	0.316	0.703	2.231	786.232	623.683
EIF1AY	0.489	0.808	2.161	467.382	411.143
KDM5D	0.159	0.563	1.965	1123.460	847.623
GDF15	0.000	0.000	1.955	197.445	42.331
NAALAD2	0.017	0.324	1.493	59.147	38.962
PCDH9	0.017	0.323	1.307	1643.213	1028.235
TXLNGY	0.081	0.466	1.286	491.766	342.247
TRAT1	0.080	0.466	1.274	293.752	218.858

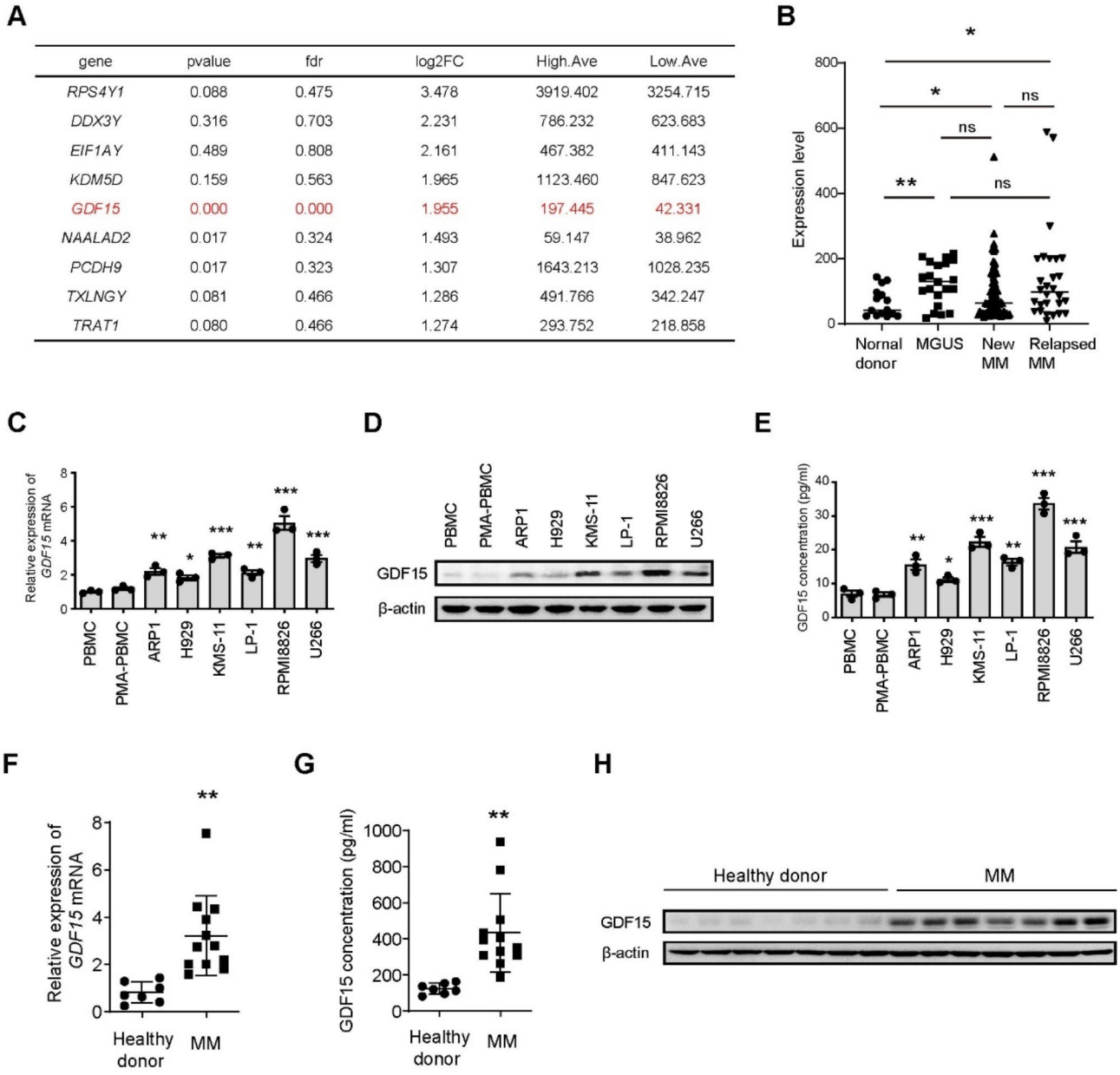

Fig. 1 GDF15 is identified as a differentially expressed gene in MM. (**A**) Differential analysis showed the genes upregulated in MM tissues, ranked by fold change. Data was derived from GSE6477 dataset. (**B**) GDF15 expression level in samples from normal donor ($n=15$), MGUS ($n=21$), newly diagnosed MM ($n=75$), and relapsed MM ($n=28$). (**C**) Real-time qPCR showed *GDF15* mRNA level in MM cell lines and healthy control cells ($n=3$ per group). (**D**) Western blotting showed GDF15 protein level in MM cell lines and healthy control cells. (**E**) ELISA showed secreted GDF15 level in MM cell lines and healthy control cells ($n=3$ per group). (**F**) Real-time qPCR showed *GDF15* mRNA level in samples from 12 MM patients and 7 healthy donors. (**G**) ELISA showed secreted GDF15 level in serum samples from 12 MM patients and 7 healthy donors. (**H**) ELISA showed GDF15 protein level in serum samples from 7 MM patients and 7 healthy donors. Experiments in **C**-**E** were repeated two times, while experiments in **F**-**H** were not repeated. *P* values were calculated using unpaired two-tailed Student's t-test or one-way ANOVA for Tukey's multiple-comparisons test. $^{*}P<0.05$, $^{**}P<0.01$, $^{***}P<0.001$; ns, not significant

significantly among patients with MGUS, newly diagnosed MM, and relapsed MM (Fig. 1B). Next, we investigated GDF15 expression in a series of MM cell lines. We observed that compared to normal PBMC, the mRNA level of *GDF15* was highly expressed in MM cells (ARP1, H929, KMS-11, LP-1, RPMI8826, and U266) (Fig. 1C). This finding was confirmed by Western blotting, which showed that H929 cells had the lowest GDF15 protein level, while RPMI8826 cells had the highest GDF15 protein level (Fig. 1D). Additionally, ELISA demonstrated a similar expression pattern in the secreted level of GDF15 (Fig. 1E).

To further verify the expression pattern of GDF15 in clinical samples, we compared GDF15 expression in 12 MM patients and 7 healthy donors. Both real-time qPCR and ELISA revealed that GDF15 was highly expressed in MM compared to normal controls (Fig. 1F-G). Additionally, western blotting showed that the GDF15 protein level was much higher in MM samples ($n = 7$) compared to healthy controls ($n = 7$) (Fig. 1H). These findings collectively indicate that GDF15 is highly expressed in MM and may act as a tumor promoter.

GDF15 exhibits growth-promoting and anti-apoptotic roles in MM

To investigate the potential oncogenic roles of GDF15 in MM, we conducted gain-of-function and loss-of-function studies. RPMI8826 cells were selected for loss-of-function experiments, while H929 cells were chosen for gain-of-function experiments (Fig. 2A-B). The sh*GDF15*-#1, which exhibited high knockdown efficiency, was utilized for further investigation. Using the CCK-8 assay, we demonstrated that genetic silencing of *GDF15* inhibited cell proliferation in RPMI8826 cells, whereas overexpression of *GDF15* promoted cell proliferation in H929 cells (Fig. 2C). Under serum starvation conditions, the cell apoptosis ratio of RPMI8826 cells was significantly increased by *GDF15* knockdown, while the apoptosis of H929 cells was reduced by *GDF15* overexpression (Fig. 2D). Furthermore, by utilizing recombinant human GDF15 protein (rGDF15), we observed that rGDF15 significantly promoted the cell proliferation of H929 cells and protected them from starvation-induced apoptosis (Fig. 2E-F). These findings collectively suggest that GDF15 is involved in the regulation of MM cell proliferation and apoptosis.

GDF15 induces glycolytic metabolism in MM cells

To unravel the underlying cellular mechanism of GDF15 in MM, we conducted an analysis of GDF15-related molecular events. For this purpose, we performed gene set enrichment analysis in GSE6477 based on the median expression value of *GDF15* mRNA level. Using the HALLMARK gene sets, we observed that GDF15 was associated with numerous signaling cascades, particularly HALLMARK_GLYCOLYSIS, HALLMARK PANCREAS BETA CELLS, HALLMARK EPITHELIAL MESENCHYMAL TRANSITION, and HALLMARK_TGF_BETA_SIGNALING (Fig. 3A). Given the significant changes in glycolysis, we subsequently investigated the potential implication of GDF15 on the Warburg effect of MM cells.

We conducted experiments to assess the impact of genetic manipulation of GDF15 on glucose consumption and lactate production by harvesting the culture medium. Our findings revealed that both glucose uptake and lactate production were decreased upon *GDF15* knockdown, while the opposite results were observed with *GDF15* overexpression (Fig. 3B-C). Additionally, we utilized the Seahorse XF24 Extracellular Flux Analyzer to analyze the extracellular acidification rate (ECAR) and oxygen consumption rate (OCR). For the ECAR analysis, we presented ECARmax and glycolytic reserve. In the OCR analysis, OCRmax and spare respiratory capacity (SRC) were normalized to the non-mitochondrial respiration to account for the influence of other non-mitochondrial sources of oxygen consumption. The results demonstrated that *GDF15* knockdown significantly inhibited the glycolytic capacity of RPMI8226 cells, while oxidative phosphorylation, indicated by OCRmax and SRC, was enhanced (Fig. 3D). Conversely, *GDF15* overexpression induced a metabolic shift from oxidative phosphorylation to fermentation, as evidenced by increased ECAR and reduced OCR (Fig. 3E). The effects induced by *GDF15* overexpression were mirrored by rGDF15, which also promoted the Warburg-like metabolism of H929 cells, as evidenced by increased glucose uptake, lactate production, ECAR, and OCR (Fig. 3F-H).

To determine whether the cellular functions of GDF15 are dependent on enhanced glycolysis, we blocked glycolysis pathway with 2-Deoxy-D-glucose (2-DG). As a result, 2-DG largely mitigated the pro-proliferation and anti-apoptotic effects induced by *GDF15* overexpression (Fig. 3I-J). Collectively, these findings suggest that GDF15 may enhance glycolysis to support its oncogenic activities in MM cells.

GDF15 promotes the expression of glycolytic genes in MM cells

To investigate how GDF15 enhances glycolysis in MM, we analyzed several key glycolytic components, including hexokinase 2 (HK2), pyruvate kinase M2 (PKM2), lactate dehydrogenase A (LDHA), and the glucose transporter GLUT1 (encoded by the *SLC2A1* gene). Real-time qPCR analysis revealed that *GDF15* knockdown led to reduced expression of these genes, with the most notable impact observed on *SLC2A1* mRNA. In contrast, GDF15 overexpression or treatment with rGDF15 stimulated the

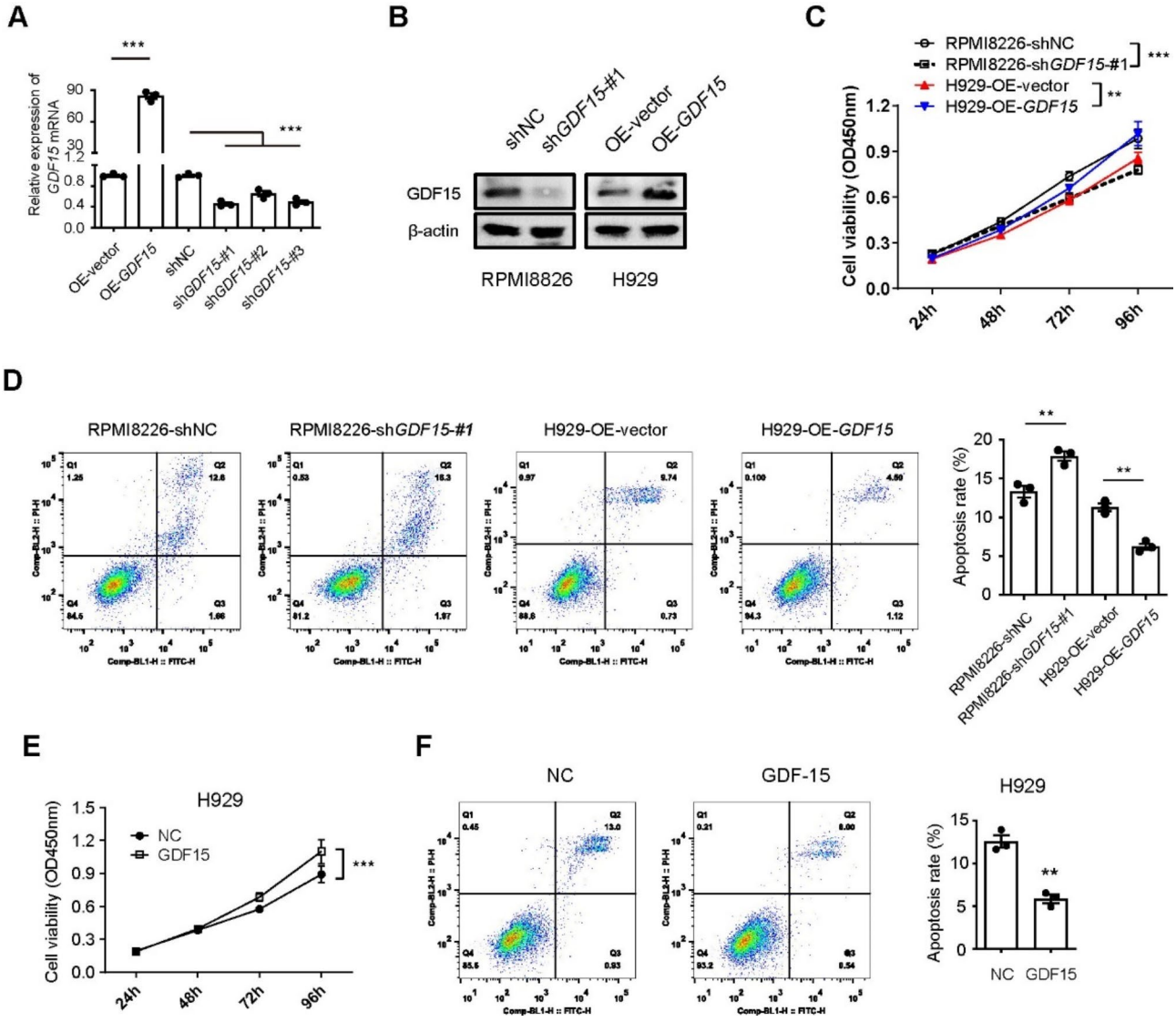

Fig. 2 GDF15 exhibits growth-promoting and anti-apoptotic roles in MM.(**A**) Real-time qPCR showed the *GDF15* mRNA level in MM cells (RPMI8826 and H929) with GDF15 knockdown or overexpression ($n=3$ per group). (**B**) Western blotting showed the GDF15 protein level in MM cells (RPMI8826 and H929) with GDF15 knockdown or overexpression. (**C**) CCK-8 assay showed the effects of *GDF15* knockdown or overexpression on the cell proliferation of RPMI8826 or H929 cells ($n=3$ per group). (**D**) Annexin V/PI staining assay showed the effects of *GDF15* knockdown or overexpression on the cell apoptosis of RPMI8826 or H929 cells under serum starvation ($n=3$ per group). (**E**) CCK-8 assay showed the effects of recombinant GDF15 protein on the cell proliferation of H929 cells ($n=3$ per group). (**F**) Annexin V/PI staining assay showed the effects of recombinant GDF15 protein on the cell apoptosis of H929 cells under serum starvation ($n=3$ per group). All experiments were repeated two times. *P* values were calculated using unpaired two-tailed Student's t-test. $^{**}P<0.01$, $^{***}P<0.001$

expression of these glycolytic genes (Fig. 4A). Consistent with the mRNA data, western blotting confirmed the stimulatory effects of GDF15 on the protein expression of these glycolytic enzymes and the glucose transporter (Fig. 4B).

Recently, several studies have suggested that GDF15 binds with TGFβRII and activates downstream SMAD2/3 pathways [24, 25]. The expression of glycolytic genes induced by GDF15, including *PKM2*, *SLC2A1*, *HK2*, and *LDHA*, shows a pattern that is indeed similar to the expression profiles observed with TGFβ stimulation (Supplementary Fig. 1). Additionally, we observed a close association between the activation of the TGFβ signaling pathway and GDF15 expression (Fig. 4C). Therefore, we conducted further tests to examine the link between GDF15 and the TGFβ signaling pathway in MM cells. Western blotting results showed that the phosphorylated levels of Smad2 and Smad3, indicators of TGFβ signaling activation, were reduced by *GDF15* knockdown in RPMI8226 cells, while increased by GDF15 overexpression or treatment with rGDF15 in H929 cells (Fig. 4D).

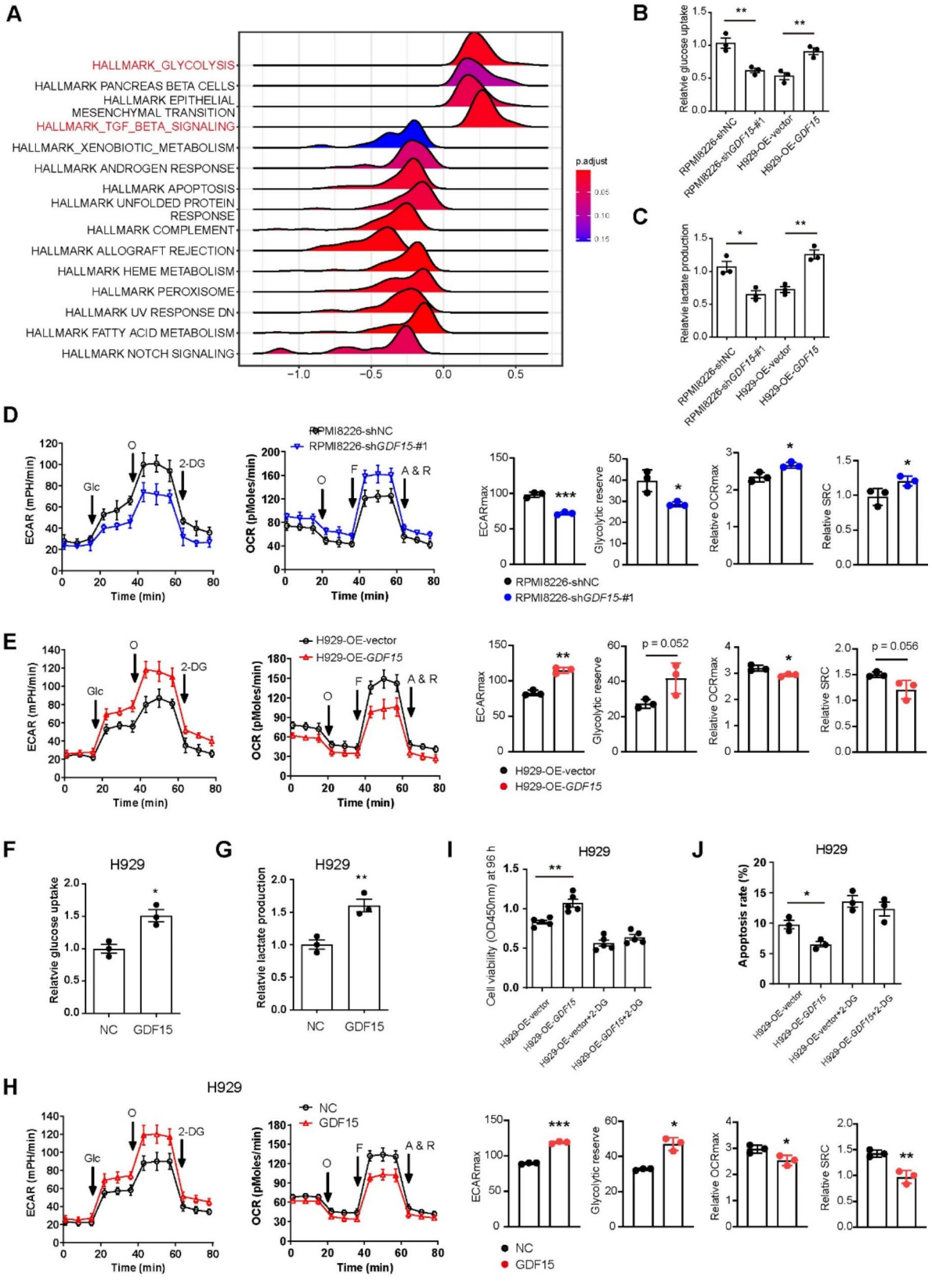

Fig. 3 (See legend on next page.)

(See figure on previous page.)

Fig. 3 GDF15 induces glycolytic metabolism in MM cells. (**A**) GSEA showed the cellular events related to GDF15 expression. The GSE6477 dataset and the HALLMARK gene sets were used for analysis. (**B**) The effects of *GDF15* knockdown or overexpression on the glucose consumption of RPMI8826 or H929 cells. (**C**) The effects of *GDF15* knockdown or overexpression on the lactate production of RPMI8826 or H929 cells. (**D**) Seahorse analysis showed the effects of *GDF15* knockdown on the ECAR and OCR of RPMI8826 cells. (**E**) Seahorse analysis showed the effects of *GDF15* overexpression on the ECAR and OCR of H929 cells. (**F**) The effects of recombinant GDF15 protein on the glucose consumption of H929 cells. (**G**) The effects of recombinant GDF15 protein on the lactate production of H929 cells. (**H**) Seahorse analysis showed the effects of recombinant GDF15 protein on the ECAR and OCR of H929 cells. (**I**) CCK-8 assay showed the effects of *GDF15* overexpression on the cell proliferation of H929 cells in the presence or absence of 2-DG. (**J**) Annexin V/PI staining assay showed the effects of *GDF15* overexpression on the cell apoptosis H929 cells under serum starvation in the presence or absence of 2-DG. For ECAR and OCR analysis, OCRmax, SRC, ECARmax, and glycolytic reserve were calculated; OCRmax and SRC were normalized to the non-mitochondrial respiration. Experiments in **B-J** were repeated two times and data were generated with three replicates. *P* values were calculated using unpaired two-tailed Student's t-test. $^{*}P < 0.05$, $^{**}P < 0.01$. Glc, glucose; 2-DG, 2-deoxy-d-glucose; O, oligomycin; F, carbonyl cyanide-p-trifluoromethoxyphenylhydrazone (FCCP); A&R, rotenone/antimycin A; SRC, spare respiratory capacity

These findings suggest that GDF15 can indeed activate the TGFβ signaling pathway.

The oncogenic activities of GDF15 are dependent on the activation of TGFβ signaling pathway

To interrogate whether the activation of the TGFβ signaling pathway is essential for the functions of GDF15 in MM cells, we pharmacologically inhibited the TGFβ signaling pathway using a small molecule inhibitor, LY2109761. Through CCK-8 assay, we demonstrated that the increased cell proliferation induced by *GDF15* overexpression was effectively reduced by LY2109761 in H929 cells (Fig. 5A). Similarly, the anti-apoptotic role of GDF15 in H929 cells was abrogated by LY2109761 (Fig. 5B). We repeated these experiments with rGDF15 and found similar results when LY2109761 was used (Fig. 5C-D).

Furthermore, we examined the effects of LY2109761 on MM cell glycolysis. As illustrated in Fig. 5E-H, the stimulatory effects of GDF15 on glucose uptake, lactate production, ECAR, and OCR were significantly inhibited by LY2109761. Similarly, the enhanced glycolysis induced by rGDF15 was also suppressed by LY2974002 (Fig. 5I-L). In summary, these findings strongly suggest that GDF15 modulates MM cell functions, encompassing cell proliferation, apoptosis, and glycolysis, through the regulation of the TGFβ signaling pathway.

Transcriptional regulation of SLC2A1 by GDF15-TGFβ signaling cascades in MM

The TGFβ signaling pathway is known to activate the expression of multiple glycolytic genes in various cellular systems [26, 27]. In this study, we focused on the study of SLC2A1 due to its significant influence by GDF15. We observed that the upregulation of SLC2A1 induced by *GDF15* overexpression or rGDF15 was effectively suppressed by LY2109761, as confirmed by real-time qPCR (Fig. 6A) and western blotting analysis (Fig. 6B). The mRNA levels of *PKM2*, *HK2*, and *LDHA* induced by GDF15 were reduced to varying extents by treatment with LY2109761 (Supplementary Fig. 2).

To investigate the transcriptional regulation of *SLC2A1* expression by the Smad complex, we selected the DNA sequence of the *SLC2A1* transcription start site $-2000 \sim +222$, which was predicted to contain multiple binding sites for Smad2. Subsequently, we designed four pairs of primers for different segments, and the purified DNA after ChIP was analyzed using qPCR, revealing a significant enrichment in the P4 segment (Fig. 6C). Additionally, a luciferase reporter experiment was conducted to further confirm the regulatory effect of the Smad complex on the expression of the *SLC2A1* gene. The results indicated that the promoter activity of different segments was comparable (Fig. 6D), suggesting that the transcriptional regulatory activity primarily resides in the $-500 \sim +222$ segment.

As a second line of evidence, we genetically silenced Smad2 and observed a marked reduction in *SLC2A1* expression following Smad2 knockdown (Fig. 6E). This finding was further confirmed by western blotting analysis (Fig. 6F). Notably, the luciferase reporter assay demonstrated that Smad2 interference can down-regulate the stimulatory effect of GDF15 on the *SLC2A1* promoter activity (Fig. 6G). These data collectively support the notion that GDF15 can induce *SLC2A1* expression through Smad complex-dependent transcriptional regulation.

GDF15 promotes tumor growth of MM cells in vivo

To further validate the oncogenic roles in an in vivo setting, we established a subcutaneous xenotransplanted tumor model using human MM cells in nude mice. Each mouse was administered a subcutaneous injection of 1×10^6 RPMI8226 or H929 cells with either *GDF15* knockdown or overexpression. Consistent with the results observed in the in vitro experiments, GDF15 knockdown led to a significant reduction in the growth of tumors formed by RPMI8226 cells, while *GDF15* overexpression resulted in the promotion of tumor growth in H929 cell-formed tumors (Fig. 7A). This was evidenced by the analysis of tumor growth curves and the measurement of final tumor weight (Fig. 7B-C). We also measured the serum levels of GDF15 in above animal models and found no significant difference in GDF15 levels between the treatment

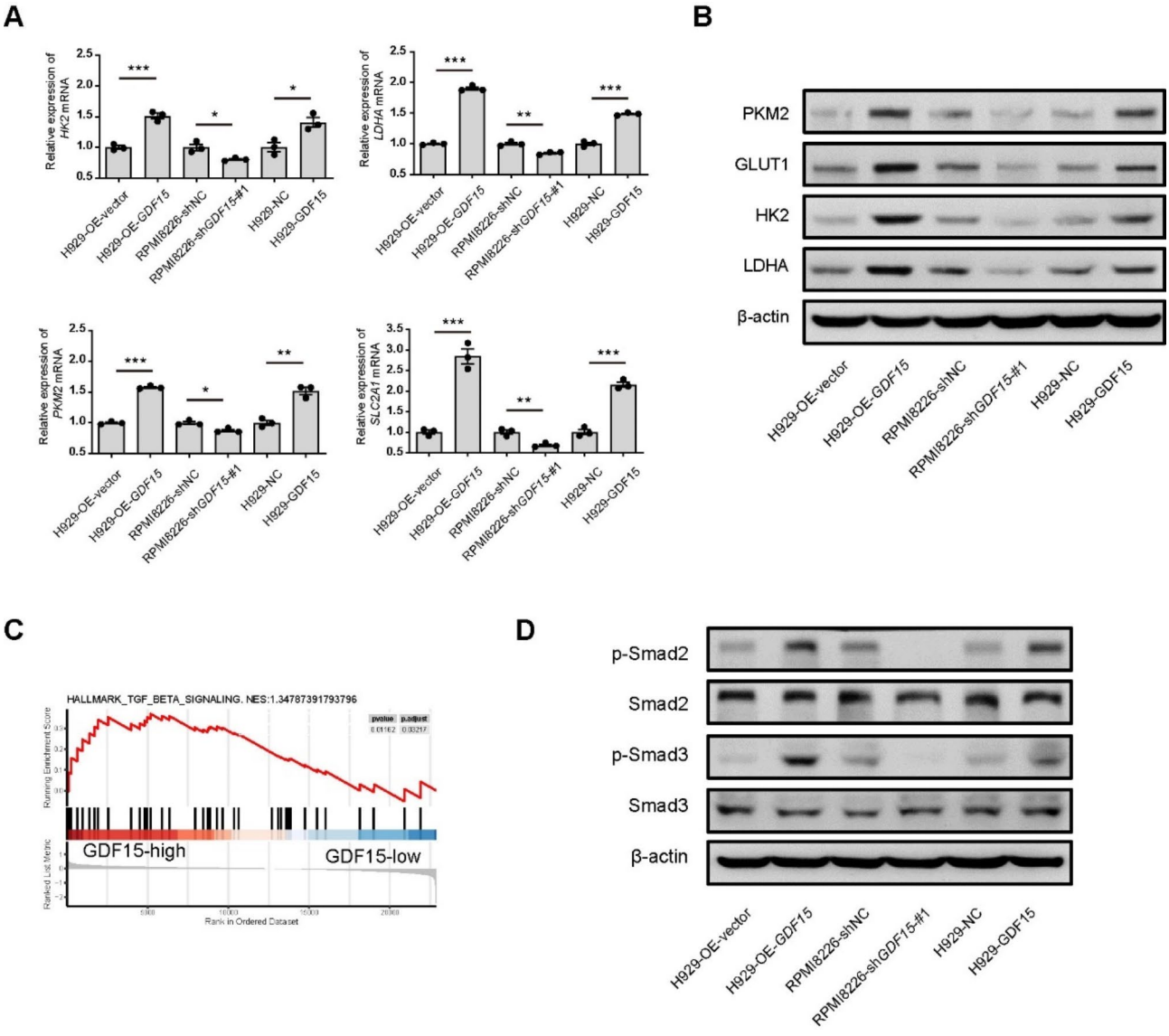

Fig. 4 GDF15 promotes the expression of glycolytic genes in MM cells. (**A**) Real-time qPCR analysis showed the effects of *GDF15* knockdown, *GDF15* overexpression, and rGDF15 on the mRNA expression of glycolytic genes in RPMI8826 and H929 cells ($n = 3$ per group). (**B**) Western blotting showed the effects of *GDF15* knockdown, *GDF15* overexpression, and rGDF15 on the protein expression of glycolytic genes in RPMI8826 and H929 cells. (**C**) GSEA plot of TGFβ signaling pathway, enriched based on the median expression of GDF15 in the GSE6477 dataset. (**D**) Western blotting showed the effects of *GDF15* knockdown, *GDF15* overexpression, and rGDF15 on the activation of TGFβ signaling pathway, as indicated by p-Samd2 and p-Samd3. Experiments in **A**, **B**, **D** were repeated two times. *P* values were calculated using unpaired two-tailed Student's t-test. $^{*}P < 0.05$, $^{**}P < 0.01$, $^{***}P < 0.001$

and control groups. This indicates that the observed decrease in MM cell proliferation upon genetic modification of GDF15 is not due to variations in GDF15 serum levels, but rather indicates a local effect (Supplementary Fig. 3). Furthermore, we tested the therapeutic efficacy of GDF15 neutralizing antibody using the subcutaneous xenotransplanted tumor model with RPMI8226 cells. Consistently, neutralizing GDF15 significantly inhibited tumor growth (Fig. 7D-F).

Discussion

Previous research has demonstrated that GDF15 is a versatile molecule capable of regulating various biological processes, including bone remodeling, hematopoiesis, energy homeostasis, adipocyte metabolism, and response to diverse stress signals [20, 28–33]. In the context of tumors, the role of GDF15 is also complex and depends on the specific cancer type, disease stage, and tumor microenvironment. In the context of tumors, GDF15 has been observed to have a multifaceted impact on promoting cancer. Its effects encompass various aspects such as facilitating tumor growth,

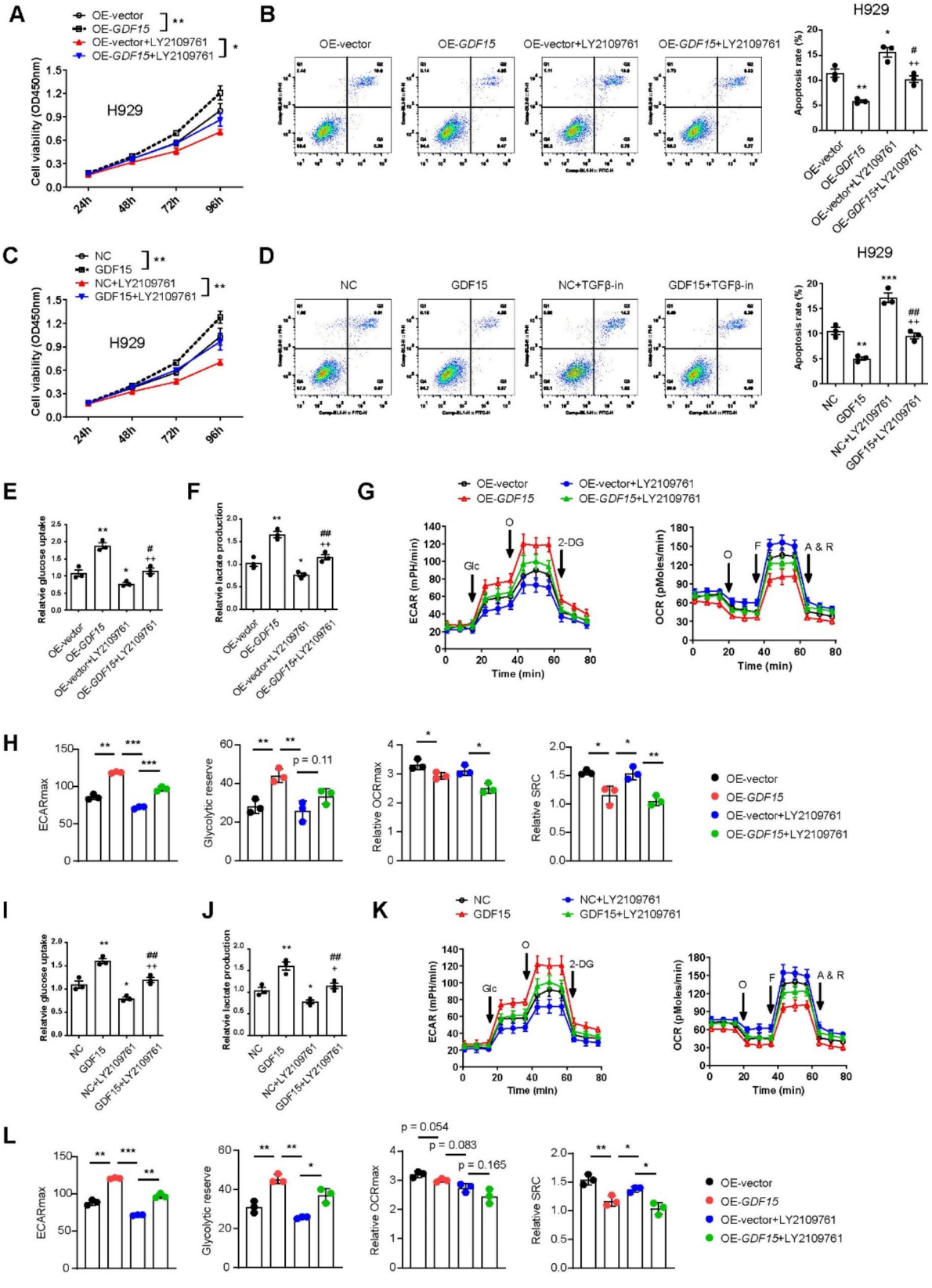

Fig. 5 (See legend on next page.)

(See figure on previous page.)

Fig. 5 The oncogenic activities of GDF15 are dependent on the activation of TGFβ signaling pathway. (**A**) CCK-8 assay showed the effects of *GDF15* overexpression on the cell proliferation of H929 cells in the presence or absence of LY2109761. (**B**) Annexin V/PI staining assay showed the effects of *GDF15* overexpression on the cell apoptosis of H929 cells under serum starvation in the presence or absence of LY2109761. vs. OE-vector: $^{*}P<0.05$, $^{**}P<0.01$; vs. OE-*GDF15*: $^{++}P<0.01$; vs. OE-vector + LY2109761: $^{\#}P<0.05$. (**C**) CCK-8 assay showed the effects of rGDF15 on the cell proliferation of H929 cells in the presence or absence of LY2109761. (**D**) Annexin V/PI staining assay showed the effects of rGDF15 on the cell apoptosis of H929 cells under serum starvation in the presence or absence of LY2109761. vs. NC: $^{**}P<0.01$, $^{***}P<0.001$; vs. GDF15: $^{++}P<0.01$; vs. GDF15 + LY2109761: $^{\#\#}P<0.01$. (**E-G**) The effects of *GDF15* overexpression on the glucose uptake, lactate production, ECAR, and OCR changes of H929 cells in the presence or absence of LY2109761. vs. OE-vector: $^{*}P<0.05$, $^{**}P<0.01$; vs. OE-*GDF15*: $^{++}P<0.01$; vs. OE-vector + LY2109761: $^{\#}P<0.05$, $^{\#\#}P<0.01$. (**H**) Statistics for ECARmax, glycolytic reserve, OCRmax, and SRC in **G**. OCRmax and SRC were normalized to the non-mitochondrial respiration. (**I-K**) The effects of rGDF15 on the glucose uptake, lactate production, ECAR, and OCR changes of H929 cells in the presence or absence of LY2109761. vs. NC: $^{**}P<0.01$; vs. GDF15: $^{+}P<0.05$, $^{++}P<0.01$; vs. GDF15 + LY2109761: $^{\#\#}P<0.01$. (**L**) Statistics for ECARmax, glycolytic reserve, OCRmax, and SRC in **K**. OCRmax and SRC were normalized to the non-mitochondrial respiration. All experiments were conducted three times, and data from each experiment were generated using three replicates. *P* values were calculated using unpaired two-tailed Student's t-test or one-way ANOVA for Tukey's multiple-comparisons test. $^{*}P<0.05$, $^{**}P<0.01$, $^{***}P<0.001$. Glc, glucose; 2-DG, 2-deoxy-d-glucose; O, oligomycin; F, carbonyl cyanide-p-trifluoromethoxyphenylhydrazone (FCCP); A&R, rotenone/antimycin A; SRC, spare respiratory capacity

promoting metastasis, contributing to drug resistance, aiding in immune escape mechanisms, and influencing changes in the tumor microenvironment [34–36]. These diverse roles underscore the complex involvement of GDF15 in the progression and behavior of cancerous growths. In this study, we broaden the understanding of GDF15's role in regulating cancer metabolism and elucidate the cellular mechanisms through which it exerts its oncogenic effects in MM.

Historically, numerous independent studies have consistently reported that the glial cell line-derived neurotrophic factor (GDNF) family receptor α-like (GFRAL) serves as the receptor for GDF15. The three-dimensional structure study also indicates a high affinity between GDF15 and GFRAL, underscoring the significance of their interaction [37, 38]. Furthermore, it has been demonstrated that the functionality of GDF15 is contingent upon its binding with GFRAL, particularly in the regulation of body weight and cancer-associated cachexia [39, 40]. Our research has revealed a novel aspect of GDF15's functionality, demonstrating its ability to activate the TGFβ signaling pathway in a manner distinct from the classical receptor action of GFRAL. This significant finding is underpinned by the bioinformatics analysis, followed by validation with western blotting. Despite being a divergent member of the TGFβ superfamily, GDF15 has been shown not to directly bind with the TGFβ receptor, as evidenced by previous studies [24, 25]. Instead, it forms a binding interaction with the GFRAL receptor. For instance, upon GDF15 binding, GFRAL engages with its co-receptor, RET, leveraging the signals of ERK and AKT [41]. However, it is important to note that some studies also support the notion that GDF15 can activate the TGFβ signaling pathway through alternative mechanisms. For instance, it has been observed that GDF15 counteracts chemokine-induced neutrophil integrin activation through the ALK-5/TGFβRII heterodimer [24]. In this study, the overexpression of GDF15 or treatment with recombinant GDF15 enhanced cell viability and fermentation while reducing apoptosis. These effects were still significantly observed even in the presence of LY2109761, indicating that there may be additional pathways, beyond the TGFβ signaling pathway, contributing to the roles of GDF15 in MM. This complex interplay underscores the intricate nature of GDF15's signaling pathways and highlights the need for further investigation to fully comprehend its diverse functional roles.

This study holds promise for two potential clinical applications. Firstly, the measurement of GDF15 levels in patients' serum could serve as a valuable biomarker for both diagnosis and prediction. Previous research has indicated that while GDF15 may not significantly predict survival rates, its elevated serum concentration is closely associated with advanced stage pf MM, anemia, renal function impairment, and inflammation [22]. Additionally, following autologous stem cell transplantation, a notable decrease in GDF15 levels in MM patients suggests its potential predictive value for treatment response [42]. These findings underscore the potential utility of GDF15 as a biomarker in guiding clinical decision-making and monitoring disease progression and treatment outcomes in MM patients. Secondly, our experiments provide evidence that GDF15 can effectively suppress the growth of MM in vitro and in vivo. Currently, there is clinical research focused on GDF15, with GDF15/GFRAL being utilized as drug targets for conditions such as anorexia and cachexia [40]. Additionally, there is ongoing exploration of GDF15 neutralizing antibodies for their potential in addressing cancers [43], anti-infection measures [44], and managing the side effects caused by platinum chemotherapy [45]. Consistently, we also showed that GDF15 neutralizing antibody was effective in control MM growth. Therefore, the targeting of GDF15 holds promise for potential applications in treating MM, offering a certain level of application prospect.

In summary, our study unveils the significant role of GDF15 as a promoter of fermentation, contributing to its involvement in promoting MM. Notably, the function of GDF15 is not reliant on its classical

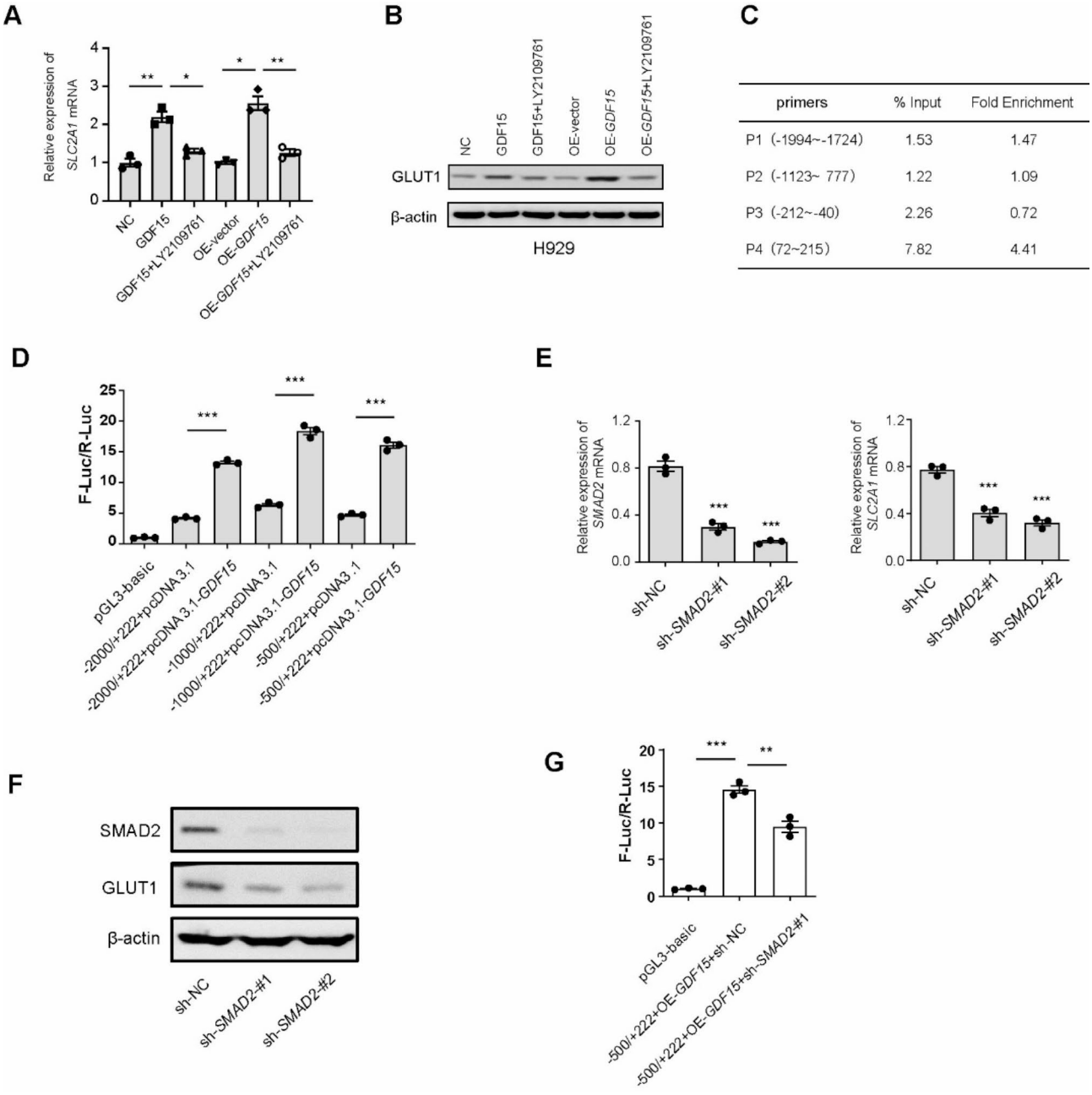

Fig. 6 Transcriptional regulation of SLC2A1 by GDF15-TGFβ signaling cascades in MM. (**A**) In H929 cells, real-time qPCR analysis showed the effects of *GDF15* overexpression or rGDF15 on the mRNA expression of SLC2A1 in the presence or absence of LY2109761 ($n = 3$ per group). (**B**) In H929 cells, western blotting showed the effects of *GDF15* overexpression or rGDF15 on the protein expression of SLC2A1 in the presence or absence of LY2109761. (**C**) CHIP experiment analysis showed the enrichment of Smad2 in the different promoter region of *SLC2A1* gene. (**D**) Luciferase reporter assay showed the promoter activity of different segments upon rGDF15 stimulation ($n = 3$ per group). (**E-F**) Real-time qPCR and western blotting analysis showed the knockdown efficiency of *SMAD2* gene and its effects on the mRNA expression of *SLC2A1* ($n = 3$ per group). (**G**) Luciferase reporter assay showed the *SLC2A1* promoter activity upon *GDF15* overexpression and *SMAD2* knockdown ($n = 3$ per group). All experiments were repeated two times. *P* values were calculated using unpaired two-tailed Student's t-test or one-way ANOVA for Tukey's multiple-comparisons test. $^{*}P < 0.05$, $^{**}P < 0.01$, $^{***}P < 0.001$

receptor GFRAL, but rather operates through the activation of the TGFβ signaling pathway. The TGFβ signal cascades govern the expression of glycolytic genes through the Samd transcription complex, leading to the enhancement of the Warburg effect. This study further broadens our understanding of the role and mechanism of GDF15 in tumors, thereby providing a foundational basis for its potential targeting in MM treatment.

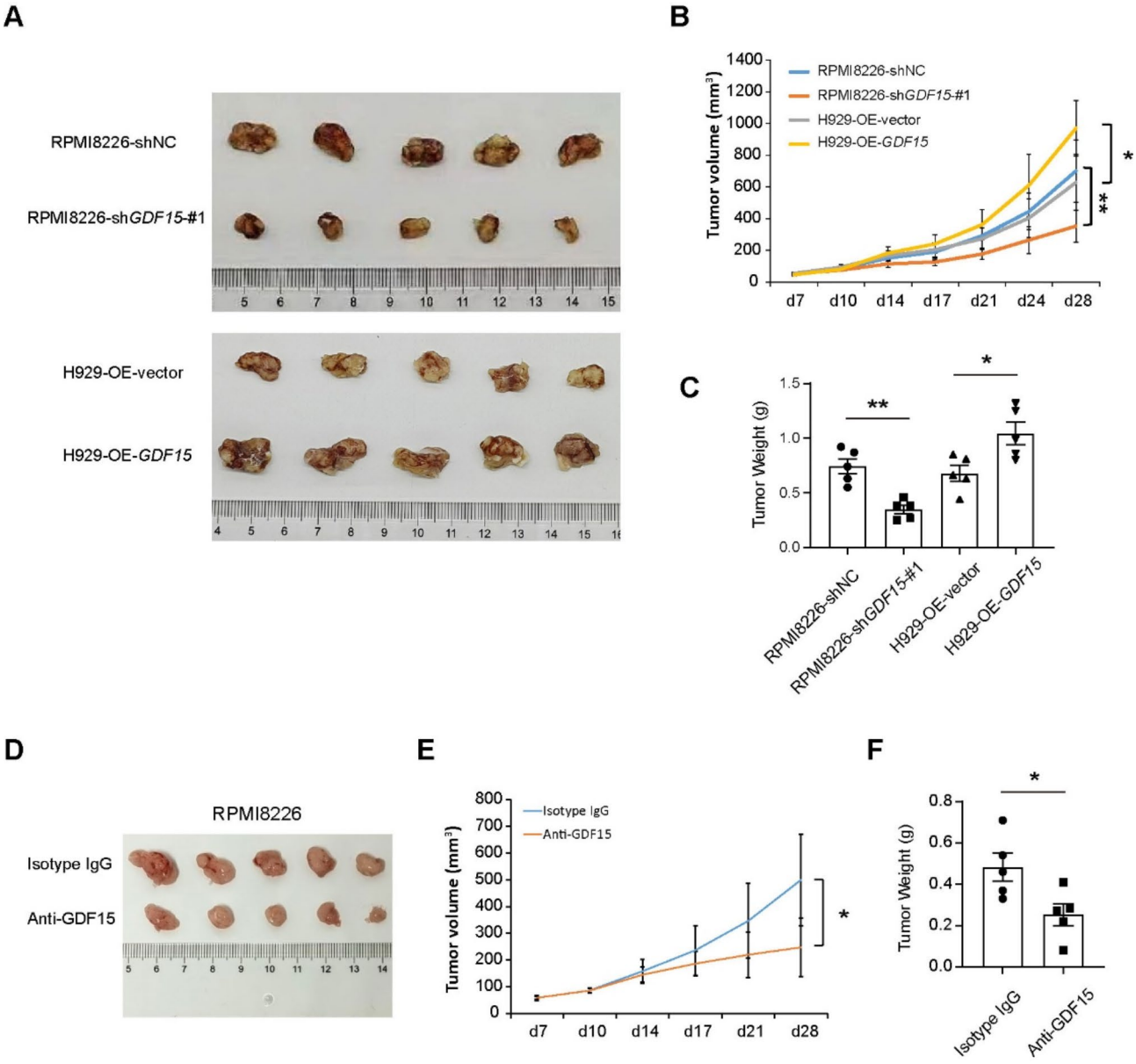

Fig. 7 GDF15 promotes tumor growth of MM cells in vivo. (**A**) The subcutaneous xenotransplanted tumors formed from RPMI8226 or H929 cells with either *GDF15* knockdown or overexpression ($n=5$ per group). (**B-C**) The growth curves and tumor weight of tumors formed from RPMI8226 or H929 cells with either *GDF15* knockdown or overexpression ($n=5$ per group). (**D**) The subcutaneous xenotransplanted tumors formed from RPMI8226 with treatment of GDF15 neutralizing antibody or isotype IgG ($n=5$ per group). (**E-F**) The growth curves and tumor weight of tumors formed from RPMI8226 with treatment of GDF15 neutralizing antibody or isotype IgG ($n=5$ per group). All animal experiments were independently conducted two times. *P* values were calculated using unpaired two-tailed Student's t-test or two-way ANOVA for Tukey's multiple-comparisons test. $^{*}P<0.05$, $^{**}P<0.01$

Supplementary Information

The online version contains supplementary material available at https://doi.org/10.1186/s40170-025-00373-7.

Supplementary Material 1

Acknowledgements
This work was supported by grants from Fudan University Affiliated Jinshan Hospital youth Research Fund (JYQN- JC-202305).

Author contributions
Manuscript conceptualization: Wenjing Xue, Feng Zhang; Data curation, formal analysis, methodology, software, validation, writing original draft: Wenjing Xue, Ying Li; Figures drawing: Yanna Ma. Final manuscript review and editing: all authors.

Data availability
No datasets were generated or analysed during the current study.

Declarations

Competing interests
The authors declare no competing interests.

Received: 13 June 2024 / Accepted: 10 January 2025
Published online: 27 January 2025

References

1. Koppenol WH, Bounds PL, Dang CV. Otto Warburg's contributions to current concepts of cancer metabolism, Nature reviews. Cancer. 2011;11:325–37.
2. Vander Heiden MG, Cantley LC, Thompson CB. Understanding the Warburg effect: the metabolic requirements of cell proliferation. Science. 2009;324:1029–33.
3. Chen PC, Ning Y, Li H, Su JG, Shen JB, Feng QC, Jiang SH, Shi PD, Guo RS. Targeting ONECUT3 blocks glycolytic metabolism and potentiates anti-PD-1 therapy in pancreatic cancer. Cell Oncol. 2024;47:81–96.
4. Stine ZE, Schug ZT, Salvino JM, Dang CV. Targeting cancer metabolism in the era of precision oncology. Nat Rev Drug Discovery. 2022;21:141–62.
5. Barba I, Carrillo-Bosch L, Seoane J. Targeting the Warburg Effect in Cancer: where do we stand? Int J Mol Sci, 25 (2024).
6. Dutta AK, Alberge JB, Sklavenitis-Pistofidis R, Lightbody ED, Getz G, Ghobrial IM. Single-cell profiling of tumour evolution in multiple myeloma - opportunities for precision medicine. Nat Reviews Clin Oncol. 2022;19:223–36.
7. Cowan AJ, Green DJ, Kwok M, Lee S, Coffey DG, Holmberg LA, Tuazon S, Gopal AK, Libby EN. Diagnosis and management of multiple myeloma a review. Jama-J Am Med Assoc. 2022;327:464–77.
8. Li L, Hu XY, Nkwocha J, Sharma K, Kmieciak M, Mann H, Zhou L, Grant S. Non-canonical role for the ataxia-telangiectasia-Rad3 pathway in STAT3 activation in human multiple myeloma cells. Cell Oncol. 2023;46:1369–80.
9. Dimopoulos MA, Moreau P, Terpos E, Mateos MV, Zweegman S, Cook G, Delforge M, Hájek R, Schjesvold F, Cavo M, Goldschmidt H, Facon T, Einsele H, Boccadoro M, San-Miguel J, Sonneveld P, Mey U. E.G.C. ESMO, Multiple myeloma: EHA-ESMO Clinical Practice Guidelines for diagnosis, treatment and follow-upvol 33, pg 117, (2022), Annals of Oncology, 33 (2022) 988–988.
10. Wallington-Beddoe CT, Mynott RL. Prognostic and predictive biomarker developments in multiple myeloma. J Hematol Oncol, 14 (2021).
11. Parrondo RD, Ailawadhi S, Sher T, Chanan-Khan AA, Roy V. Autologous stem-cell transplantation for multiple myeloma in the era of Novel therapies. Jco Oncol Pract. 2020;16:56–66.
12. Gavriatopoulou M, Malandrakis P, Ntanasis-Stathopoulos I, Dimopoulos MA. Nonselective proteasome inhibitors in multiple myeloma and future perspectives. Expert Opin Pharmaco. 2022;23:335–47.
13. Minnie SA, Hill GR. Immunotherapy of multiple myeloma. J Clin Invest. 2020;130:1565–75.
14. Wang DD, Day EA, Townsend LK, Djordjevic D, Jorgensen SB, Steinberg GR. GDF15: emerging biology and therapeutic applications for obesity and cardiometabolic disease. Nat Rev Endocrinol. 2021;17:592–607.
15. Siddiqui JA, Pothuraju R, Khan P, Sharma G, Muniyan S, Seshacharyulu P, Jain M, Nasser MW, Batra SK. Pathophysiological role of growth differentiation factor 15 (GDF15) in obesity, cancer, and cachexia. Cytokine Growth F R. 2022;64:71–83.
16. Rybicki BA, Chitale D, Gupta N, Jackson L, Wheeler T, Trudeau S, Jankowski M, Bobbittt K, Rundle A, Tang DL. The changing role of GDF15 (growth/differentiation factor 15) during prostate carcinogenesis. Cancer Res, 75 (2015).
17. Sadasivan SM, Chen YL, Gupta NS, Han XX, Bobbitt KR, Chitale DA, Williamson SR, Rundle AG, Tang DL, Rybicki BA. The interplay of growth differentiation factor 15 (GDF15) expression and M2 macrophages during prostate carcinogenesis. Carcinogenesis. 2020;41:1074–82.
18. Tanno T, Merchant A, Agarwal JR, Wang QJ, Matsui W. The TGF- β Family Member Growth Differentiation Factor 15 (GDF15) Regulates the Self-Renewal of Multiple Myeloma Cancer Stem Cells, Blood, 118 (2011) 1275–1275.
19. Wu Q, Ren W, Ye S, Koenigshoff M, Eickelberg O. Growth differentiation factor 15 (GDF15)-Mediated lung aging promotes human rhinovirus infection and Virus-Induced inflammation. Am J Resp Crit Care, 199 (2019).
20. Kim-Muller JY, Song LJ, Paulhus BL, Pashos E, Li XP, Rinaldi A, Joaquim S, Stansfield JC, Zhang JW, Robertson A, Pang JC, Opsahl A, Boucher M, Breen D, Hales K, Sheikh A, Wu ZD, Zhang BB. GDF15 neutralization restores muscle function and physical performance in a mouse model of cancer cachexia. Cell Rep, 42 (2023).
21. Hidman J, Larsson A, Thulin M, Karlsson T. Increased plasma GDF15 is Associated with altered levels of Soluble VEGF receptors 1 and 2 in symptomatic multiple myeloma. Acta Haematol-Basel. 2022;145:326–33.
22. Banaszkiewicz M, Malyszko J, Batko K, Koc-Zorawska E, Zorawski M, Dumnicka P, Jurczyszyn A, Woziwodzka K, Tisonczyk J, Krzanowski M, Malyszko J, Waszczuk-Gajda A, Drozdz R, Kuzniewski M, Krzanowska K. Evaluating the Relationship of GDF-15 with Clinical Characteristics, Cardinal Features, and Survival in Multiple Myeloma, Mediators of inflammation, 2020 (2020).
23. Chng WJ, Kumar S, VanWier S, Ahmann G, Price-Troska T, Henderson K, Chung TH, Kim S, Mulligan G, Bryant B, Carpten J, Gertz M, Rajkumar SV, Lacy M, Dispenzieri A, Kyle R, Greipp P, Bergsagel PL, Fonseca R. Molecular dissection of hyperdiploid multiple myeloma by gene expression profiling. Cancer Res. 2007;67:2982–9.
24. Artz A, Butz S, Vestweber D. GDF-15 inhibits integrin activation and mouse neutrophil recruitment through the ALK-5/TGF-βRII heterodimer. Blood. 2016;128:529–41.
25. Xu J, Kimball TR, Lorenz JN, Brown DA, Bauskin AR, Klevitsky R, Hewett TE, Breit SN, Molkentin JD. GDF15/MIC-1 functions as a protective and antihypertrophic factor released from the myocardium in association with SMAD protein activation. Circul Res. 2006;98:342–50.
26. Gauthier T, Yao C, Dowdy T, Jin WW, Lim YJ, Patino LC, Liu N, Ohlemacher SI, Bynum A, Kazmi R, Bewley CA, Mitrovic M, Martin D, Morell RJ, Eckhaus M, Larion M, Tussiwand R, O'Shea JJ, Chen WJ. TGF-β uncouples glycolysis and inflammation in macrophages and controls survival during sepsis. Sci Signal, 16 (2023).
27. Huang YW, Chen ZC, Lu T, Bi GS, Li M, Liang JQ, Hu ZY, Zheng YS, Yin JC, Xi JJ, Lin ZW, Zhan C, Jiang W, Wang Q, Tan LJ. HIF-1α switches the functionality of TGF-β signaling via changing the partners of smads to drive glucose metabolic reprogramming in non-small cell lung cancer. J Exp Clin Canc Res, 40 (2021).
28. Zhang YY, Zhao XY, Dong XN, Zhang YY, Zou HX, Jin YG, Guo W, Zhai P, Chen X, Kharitonenkov A. Activity-balanced GLP-1/GDF15 dual agonist reduces body weight and metabolic disorder in mice and non-human primates. Cell Metabol. 2023;35:287–.
29. Benichou O, Coskun T, Gonciarz MD, Garhyan P, Adams AC, Du Y, Dunbar JD, Martin JA, Mather KJ, Pickard RT, Reynolds VL, Robins DA, Zvada SP, Emmerson PJ. Discovery, development, and clinical proof of mechanism of LY3463251, a long-acting GDF15 receptor agonist. Cell Metabol. 2023;35:274–.
30. Sokol R.J., Friederich M.W., Strode D.K., Van Hove R.A., Miller K., Gabel L., Horslen S.P., Kohli R., Lovell M.A., Miethke A., Molleston J.P., Romero R., Squires J.E., Squires R.H., Sundaram S.S., Magee J.C., Van Hove J.L.K., Network C.L.D.R. Accuracy of Gdf15 and Fgf21 to differentiate mitochondrial hepatopathies from other Pediatric Liver diseases. Hepatology. 2022;76:S200–1.
31. Klein AB, Nicolaisen TS, Johann K, Fritzen AM, Mathiesen CV, Gil C, Pilmark NS, Karstoft K, Blond MB, Quist JS, Seeley RJ, Færch K, Lund J, Kleinert M, Clemmensen C. The GDF15-GFRAL pathway is dispensable for the effects of metformin on energy balance. Cell Rep, 40 (2022).
32. He RZ, Shi JJ, Xu DP, Yang J, Shen Y, Jiang YS, Tao LY, Yang MW, Fu XL, Yang JY, Liu DJ, Huo YM, Shen XQ, Lu P, Niu NN, Sun YW, Xue J. SULF2 enhances GDF15-SMAD axis to facilitate the initiation and progression of pancreatic cancer. Cancer Lett, 538 (2022).
33. Katsumura S, Siddiqui N, Goldsmith MR, Cheah JH, Fujikawa T, Minegishi G, Yamagata A, Yabuki Y, Kobayashi K, Shirouzu M, Inagaki T, Huang THM, Musi N, Topisirovic I, Larsson O, Morita M. Deadenylase-dependent mRNA decay of GDF15 and FGF21 orchestrates food intake and energy expenditure. Cell Metabol. 2022;34:564–.
34. Lin HP, Luo Y, Gong TY, Fang HS, Li H, Ye GY, Zhang Y, Zhong M. GDF15 induces chemoresistance to oxaliplatin by forming a reciprocal feedback loop with Nrf2 to maintain redox homeostasis in colorectal cancer. Cell Oncol, (2024).
35. Wang ZY, Wang SJ, Jia ZH, Hu YP, Cao DY, Yang MJ, Liu LG, Gao L, Qiu SM, Yan WK, Li YM, Luo J, Geng YJ, Zhang JY, Li ZZ, Wang X, Li ML, Shao R, Liu YB. YKL-40 derived from infiltrating macrophages cooperates with GDF15 to establish an immune suppressive microenvironment in gallbladder cancer. Cancer Lett, 563 (2023).
36. Joo M, Kim D, Lee MW, Lee HJ, Kim JM. GDF15 promotes cell growth, Migration, and Invasion in Gastric Cancer by Inducing STAT3 activation. Int J Mol Sci, 24 (2023).
37. Yang LD, Chang CC, Sun Z, Madsen D, Zhu HS, Padkjær SB, Wu XA, Huang T, Hultman K, Paulsen SJ, Wang JS, Bugge A, Frantzen JB, Norgaard P, Jeppesen JF, Yang ZR, Secher A, Chen HB, Li X, John LM, Shan B, He ZH, Gao X, Su J,

Hansen KT, Yang W, Jorgensen SB. GFRAL is the receptor for GDF15 and is required for the anti-obesity effects of the ligand. Nat Med. 2017;23:1158–.
38. Emmerson PJ, Wang F, Du Y, Liu Q, Pickard RT, Gonciarz MD, Coskun T, Hamang MJ, Sindelar DK, Ballman KK, Foltz LA, Muppidi A, Alsina-Fernandez J, Barnard GC, Tang JX, Liu XL, Mao XD, Siegel R, Sloan JH, Mitchell PJ, Zhang BB, Gimeno RE, Shan B, Wu XL. The metabolic effects of GDF15 are mediated by the orphan receptor GFRAL. Nat Med. 2017;23:1215–.
39. Mullican SE, Lin-Schmidt X, Chin CN, Chavez JA, Furman JL, Armstrong AA, Beck SC, South VJ, Dinh TQ, Cash-Mason TD, Cavanaugh CR, Nelson S, Huang CC, Hunter MJ, Rangwala SM. GFRAL is the receptor for GDF15 and the ligand promotes weight loss in mice and nonhuman primates. Nat Med. 2017;23:1150–.
40. Suriben R, Chen M, Higbee J, Oeffinger J, Ventura R, Li B, Mondal K, Gao ZY, Ayupova D, Taskar P, Li DN, Starck SR, Chen HIH, McEntee M, Katewa SD, Phung V, Wang M, Kekatpure A, Lakshminarasimhan D, White A, Olland A, Haldankar R, Solloway MJ, Hsu JY, Wang Y, Tang J, Lindhout DA, Allan BB. Antibody-mediated inhibition of GDF15-GFRAL activity reverses cancer cachexia in mice. Nat Med. 2020;26:1264–.
41. Xie BK, Tang WJ, Wen SA, Chen F, Yang C, Wang M, Yang Y, Liang W. GDF-15 Inhibits ADP-Induced Human Platelet Aggregation through the GFRAL/RET Signaling Complex, Biomolecules, 14 (2024).
42. Tarkun P, Atesoglu EB, Mehtap O, Musul MM, Hacihanefioglu A. Serum growth differentiation factor 15 levels in newly diagnosed multiple myeloma patients. Acta Haematol-Basel. 2014;131:173–8.
43. Wang ZW, He L, Li WN, Xu CY, Zhang JY, Wang DS, Dou KF, Zhuang R, Jin BQ, Zhang W, Hao Q, Zhang K, Zhang WQ, Wang SN, Gao Y, Gu JT, Shang L, Tan ZJ, Su HC, Zhang YQ, Zhang C, Li M. GDF15 induces immunosuppression via CD48 on regulatory T cells in hepatocellular carcinoma. J Immunother Cancer, 9 (2021).
44. Breen DM, Jagarlapudi S, Patel A, Zou C, Joaquim S, Li XP, Kang LY, Pang JC, Hales K, Ziso-Qejvanaj E, Vera NB, Bennett D, He T, Lambert M, Kelleher K, Wu ZD, Zhang BB, Lin L, Seeley RJ. O. Bezy, Growth differentiation factor 15 neutralization does not impact anorexia or survival in lipopolysaccharide-induced inflammation. Iscience; 2021. p. 24.
45. Carneiro BA, Gbolahan O, Razak AA, Hilton JF, Lambert A, Hood J, Pluta M, Bragulat V, Sanai E, Kumar R, Jodrell D, LoRusso P. Safety and efficacy of AZD8853, an anti-growth and differentiation factor 15 (GDF15) antibody, in patients (pts) with advanced/metastatic solid tumors: first-in-human study. Cancer Res, 84 (2024).

Publisher's note